ChemPubSoc Europe

DOI: 10.1002/chem.201901041

CHEMISTRY A European Journal Full Paper



Nanomaterials

# A General One-Pot Methodology for the Preparation of Mono- and Bimetallic Nanoparticles Supported on Carbon Nanotubes: Application in the Semi-hydrogenation of Alkynes and Acetylene

Diego A. Lomelí-Rosales,[a] Jorge A. Delgado,*[b] Miriam Díaz de los Bernardos,[b] Sara Pérez-Rodríguez,[b] Aitor Gual,[b] Carmen Claver,[b, c] and Cyril Godard*[c]

**Abstract:** A facile and straightforward methodology for the preparation of monometallic (copper and palladium) and bimetallic nanocatalysts (NiCu and PdCu) stabilized by a N-heterocyclic carbene ligand is reported. Both colloidal and supported nanoparticles (NPs) on carbon nanotubes (CNTs) were prepared in a one-pot synthesis with outstanding control on their size, morphology and composition. These catalysts were evaluated in the selective hydrogenation of alkynes and alkynols. **PdCu/CNTs** revealed an efficient catalytic system providing high selectivity in the hydrogenation of terminal and internal alkynes. Moreover, this catalyst was tested in the semi-hydrogenation of acetylene in industrially relevant acetylene/ethylene-rich model gas feeds and showed excellent stability even after 40 h of reaction.

## Introduction

The development of novel metal nanoparticles (MNPs) has been intensively studied in the last decades because of their unique physical and chemical properties,[1] and their potential utilization for various applications such as catalysis,[2] where their efficiency in terms of productivity is mainly attributed to their characteristic high surface-to-volume ratio compared to standard heterogeneous catalysts.[3] Such a reactivity highly depends on the size and shape of the MNPs,[4] and can be additionally modulated by the selection of the stabilizer or ligand,[2a] to provide the transformation of the substrate into a specific product.[5] In this context, the preparation of metal nanoparticles via colloidal methods can provide highly sophisticated functionalization of the active phase at structural and surface level.[3b] Moreover, colloidal nanoparticles can be utilized as models for the characterization of the active phase of catalysts, providing information which is hardly accessible when diluted onto solid carriers.

Among the transition metals reported in the selective hydrogenation of alkynes, palladium has been identified as the most efficient metal in terms of activity and selectivity.[6] Nevertheless, if the reaction is not interrupted once the alkyne substrate is consumed, pure Pd phases quickly over-hydrogenate the alkene product. The dilution of the highly active palladium phase by a second metal with a low affinity for hydrogen (e.g. Ag, Au, Cu) is one of the strategies for enhancing the catalyst performance in the selective hydrogenation of alkynes. The impact of such a dilution can be attributed to geometric and electronic effects.[6,7] The geometric effect is attributed to the creation of suitable ensembles of unique character or to the blockage of unselective active sites.[7b] The electronic effect refers to the ability of a modifier to affect the electronic properties of the active metal in order to enhance the thermodynamic selectivity and/or to suppress the formation of (sub)surface species.[6, 7c]

Among the most common bimetallic palladium-based formulations tested in the selective hydrogenation of alkynes, PdAg,[8] and PdAu,[9] revealed particularly efficient. Other combinations less extensively studied are PdPt,[9a] PtZn,[9a] PdCu,[8a] PdRhP,[10] and PdB.[11] For instance, Kiwi-Minsker and co-workers investigated the role of a second metal using colloidal Pd and bimetallic PdAg and PdCu NPs as catalysts in the selective hydrogenation of dehydroisophytol (DIP) into isophytol (IP).[8a] The bimetallic NPs were prepared using Pd/M ratios of 1.5–5.0 (M = Ag or Cu) by chemical reduction on pre-formed Pd colloids stabilized by polyvinylpyrrolidone (PVP). The bimetallic PdAg NPs adopted a core (Pd)-shell (Ag) structure whereas a mixed alloy was obtained for PdCu nanocrystals. In catalysis, a significant increase in selectivity to the target alkenol from

[a] D. A. Lomelí-Rosales
Departamento de Química
Centro Universitario de Ciencias Exactas e Ingenierías
Universidad de Guadalajara, Blvd. Marcelino García Barragán 1421
CP 44430, Guadalajara, Jalisco (México)

[b] Dr. J. A. Delgado, Dr. M. Díaz de los Bernardos, Dr. S. Pérez-Rodríguez, Dr. A. Gual, Prof. C. Claver
Centre Tecnològic de la Química, C/Marceli Domingo
43007 Tarragona (Spain)
E-mail: jorgealonso.delgado@urv.cat

[c] Prof. C. Claver, Prof. C. Godard
Departament de Química Física i Inorgànica
Universitat Rovira i Virgili, C/Marceli Domingo 1, 43007 Tarragona (Spain)
E-mail: cyril.gordard@urv.cat

Supporting information and the ORCID identification number(s) for the author(s) of this article can be found under: https://doi.org/10.1002/chem.201901041.

91% up to 97% (at 99% conversion) was observed after incorporation of the second metal. This result was attributed to the dilution of the surface Pd-sites by Ag or Cu and modification of the electronic properties of the nanoparticle surfaces.

In addition to palladium-based catalysts, very recently, Fedorov and co-workers reported the high potential of a non-noble-metal-based catalyst consisting in silica supported copper nanoparticles (capped with phosphorus or carbene ligands), in the semi-hydrogenation of alkynes.[2a,12] The authors evidenced high activity and alkene selectivity for a series of internal alkynes (at 50 bar $H_2$ and 60 °C) depending on the ligand used. In spite of these promising results, the preparation of well-defined metallic copper nanoparticles usually involves the use of expensive copper precursors and complicated synthetic methodologies.[2a,12,13] In this regard, the development of synthetic methodologies for copper nanoparticles (and bimetallic combinations of this metal) is of high interest.

Although there are available commercial options for the semi-hydrogenation of alkynes such as the Lindlar, and the more recently commercialized Pd Nanoselect catalysts, they frequently suffer from limitations in terms of robustness,[14] or accessibility.[15] In addition, the frequent requirement of the presence of large amounts of nitrogen additives or the employment of highly toxic poisons such as Pb have stimulated the research for the design of more selective and environmentally friendly catalytic systems.[3b,16]

In a previous contribution from our group, a new methodology was reported for the preparation of small and well-defined nickel nanoparticles stabilized by N-heterocyclic carbene ligand (NHC), using a "one-pot" synthesis based on the decarboxylation of 1,3-dimethylimidazolium-2-carboxylate ($Me_2ImCO_2$).[16c] The high selectivity achieved to *Z*-alkenes in the hydrogenation of alkynes using these nanocatalysts was correlated with the presence of N-heterocyclic carbene ligand (NHC) on the nickel nanoparticle surface. In the present report, this synthetic methodology was extended to other metals (Cu and Pd) and to bimetallic systems (NiCu and PdCu) and the resulting nanocatalysts applied to the liquid phase semi-hydrogenation of alkynes and the gas phase semi-hydrogenation of acetylene in ethylene-rich model gas feeds. As depicted in Scheme 1, this facile methodology, offers the possibility to access well-defined PdCu bimetallic nanostructures using a one-pot approach, offering a simple alternative to previous multistep routes.

## Results and Discussion

### Preparation of nanocatalysts

Colloidal monometallic Cu, Pd and bimetallic NiCu and PdCu were prepared by decomposition of the corresponding metallic precursors, $Cu_5Mes_5$, $Pd(dba)_2$, and mixtures of $Ni(cod)_2$/$Cu_5Mes_5$ or $Pd(dba)_2$/$Cu_5Mes_5$ respectively, under 3 bar of hydrogen in the presence of the NHC ligand precursor (0.5 equiv vs. metal).

Specific conditions of metal concentration or reaction temperature (r.t./70 °C) were utilized depending the metallic formulation (see Supporting information for details), but in all cases the reaction was carried out in a one-pot approach. Transmission electron microscopy (TEM) images of the colloidal nanoparticles are displayed in Figure 1. The series of colloidal nanoparticles exhibited in general spherical shapes, with particle sizes between 2.7–6.4 nm. The particle sizes of monometallic CuNPs and bimetallic NiCuNPs were $6.4 \pm 1.4$ and $5.2 \pm 1.1$ nm, respectively. The values obtained for the Pd and PdCu NPs were $2.7 \pm 0.5$ nm and $2.8 \pm 0.6$ nm, respectively. It is noteworthy that NPs containing Pd were smaller than those containing Cu and Ni. This observation could be explained by the faster decomposition of the palladium precursor resulting in the formation of a large number of Pd-nucleation clusters at early stages of the synthesis.

CNT-supported MNPs were also prepared following a one-pot approach via the reduction of the corresponding metallic precursors in the presence of the stabilizer and multiwalled carbon nanotubes (MWCNTs). Considering the difference of reactivity in the hydrogenation reaction of the metals deposited, catalysts with different metal loadings were prepared to facilitate the catalytic evaluation. Pd-containing catalysts were prepared at 1 wt% Pd while Ni or Cu containing materials were synthesized at 5 wt%. In all cases, the ligand to metal molar ratio employed for the synthesis was 0.5.

In a previous contribution, the effect of the NHC/Ni ratio was studied for catalysts prepared with 0.2, 0.5 and 1 equivalent of ligand per Ni.[16c] In view of the results obtained in

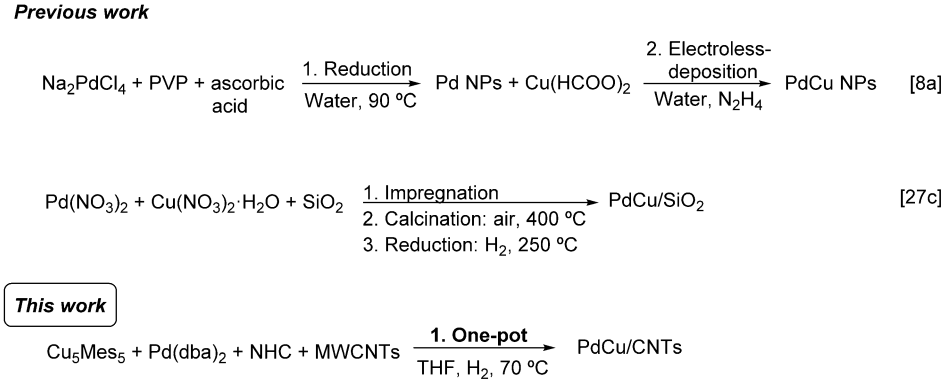


**Scheme 1.** Synthetic approaches to the preparation of PdCu bimetallic catalysts.

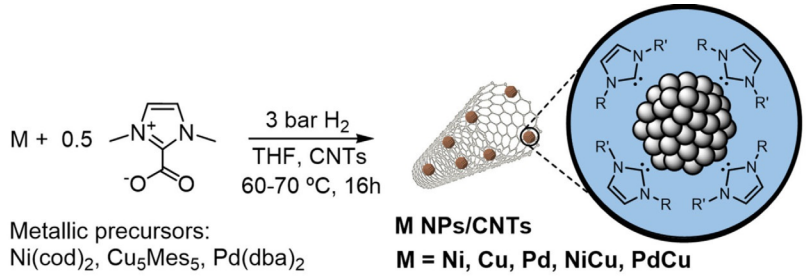


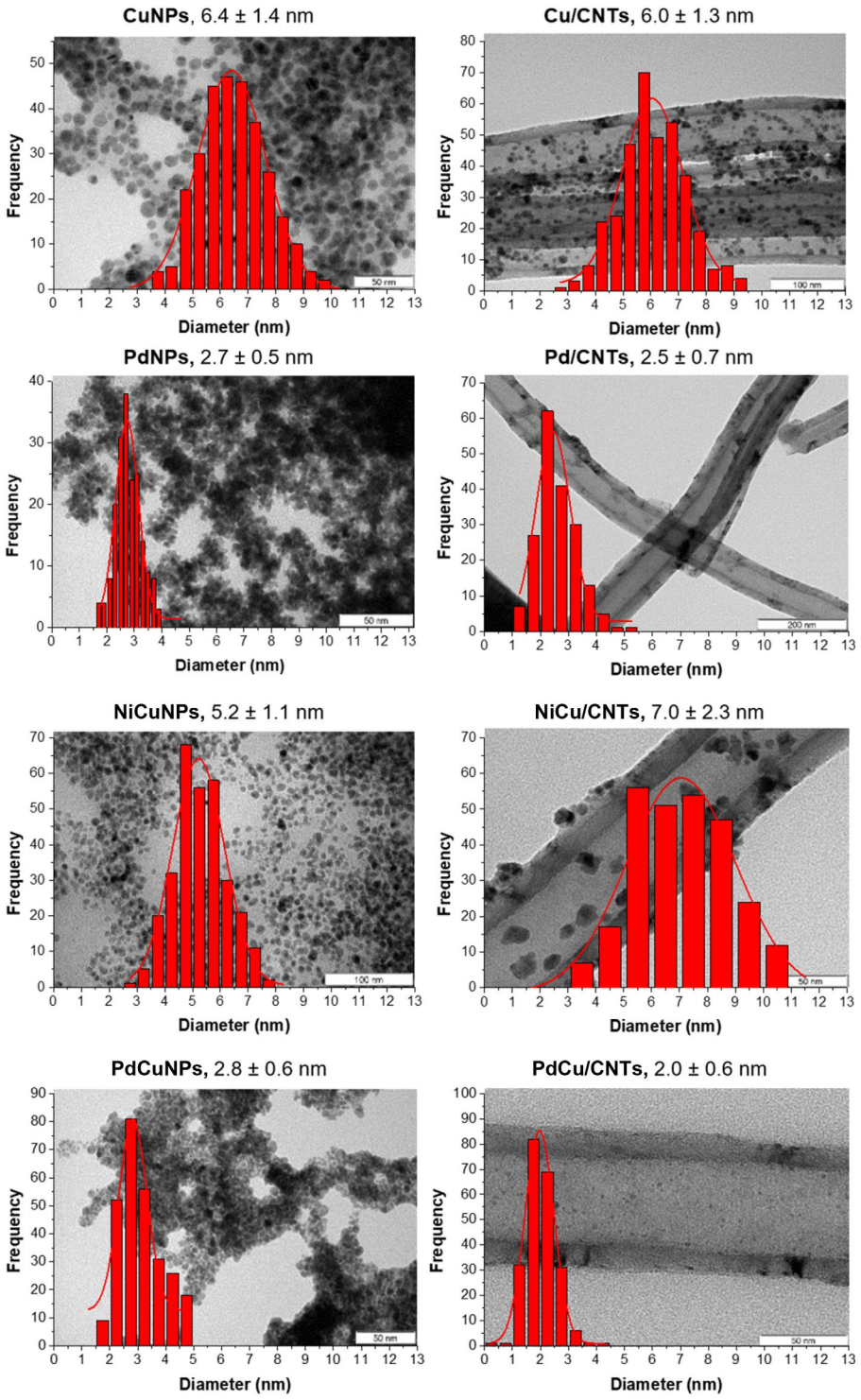


**Figure 1.** TEM images and size distributions of colloidal and CNTS supported MNPs.

terms of particle size, distribution and catalytic performance, a NHC/M ratio of 0.5 was selected in the present study.

Figure 1 displays the TEM images obtained for the colloidal M-NPs and CNT-supported nanoparticles counterparts (M-NP/CNTs). It is noteworthy that the particle sizes of colloidal and supported nanoparticles of equivalent metal formulations are similar in mean diameter and distribution, indicating that under the tested conditions, the support did not participate much in the stabilization of these nanoparticles. Similar to our observations, Karousis et al. reported similar sizes for both, colloidal and CNTs supported Pd NPs prepared by refluxing palladium acetate with SDS in water (particle sizes ca. 2–4 nm).[17]

The fine structure of the CNTs supported catalysts was studied by STEM-HAADF. Representative micrographs of each catalyst are displayed in Figure 2. In the case of **Cu/CNTs** and **Pd/CNTs**, nanoparticles of around 6.3 and 2.2 nm were observed in agreement with bright field TEM analysis. For **NiCu/CNTs**, analysis of the electron diffraction (FFT) of single NPs permitted the identification of (111) and (220) crystallographic planes which d-spacings of 2.10 and 2.80 Å, respectively. Interestingly, these spacings are slightly larger when compared to reference values of Cu-*fcc* and Ni-*fcc* phases, (see comparison in the Supporting Information), indicating an expansion of the crystalline lattice. Considering that metal nanoparticles generally show bond length contraction with the decrease in particle size, the opposite behavior could be indicative of the doping of the crystalline structure.[18] For instance, Asakura and co-workers reported the expansion of the crystalline lattice in PVP stabilized Pd NPs, a phenomena attributed to the formation of a palladium carbide phase at early stages of the synthesis of the NPs.[19] Similarly, **PdCu/CNTs** displayed d-spacings slightly larger than the values of pure Pd-*fcc*, suggesting the existence of the same phenomena observed in **NiCu/CNTs**. It is noteworthy that ideal alloyed structures should display lattice parameters or d-spacing with average values of the pure monometallic phases.

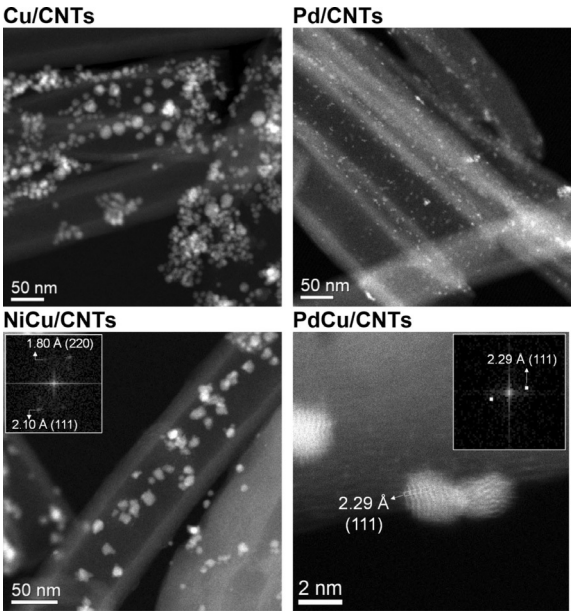


**Figure 2.** STEM-HAADF micrographs of monometallic and bimetallic CNTs supported catalysts.

The metallic composition and distribution at the nanoscale for bimetallic catalysts was studied by HAADF-STEM coupled with energy-dispersive X-ray spectroscopy (EDX). Microanalysis of single particles demonstrated the existence of both metals (Ni and Cu or Pd and Cu) in proportions similar to nominal values (see Supporting Information). The metal distribution in single NiCu and PdCu NPs was studied by EDX spectroscopy of line. According to the observed profiles (Figure 3) the distribution of both metals along the axes was consistent with bimetallic structures with uniform compositions.

The crystalline structure of the obtained nanomaterials (both, colloidal and supported catalysts), was analyzed by XRD. Due to the high sensitivity to oxidation of colloidal nanoparticles, XRD analysis were carried out under inert atmosphere. For the Cu series (Supporting Information), the colloidal nanoparticles (**CuNPs**) displayed broad bands centered at 43° and 50°, in agreement with diffractions planes (111) and (200) of metallic Cu-*fcc* structure (JCPDS: 00-004-0836). A diffraction peak at 38° was attributed to the (111) plane of cuprite possibly generated during the isolation of the NPs (JCPDS: 00-005-0667). The supported **Cu/CNTs** displayed a similar diffraction pattern than that obtained for the CNTs alone, except for an additional broadening of the band centered at 43°, due to the presence of the metallic copper phase. It is noteworthy that the absence of any feature close to 32° discards the presence of cuprite in the supported catalyst. Similarly, the **PdNPs** also displayed broad bands (in agreement with the small size of the NPs) at angles characteristic of Pd-*fcc*.

The diffractogram of the colloidal **NiCuNPs** displayed a single broad band centered at 45°(Figure 4a). This angle is the average value of the diffraction planes (111) of pure monometallic Ni and Cu-*fcc* phases, which is in agreement with an alloyed structure. The diffraction pattern observed for the **NiCu/CNTs** corresponded to the sum of the XRD profiles of the colloidal NPs and the CNTs.

For the case of the PdCu series (Figure 4b), the colloidal **PdCuNPs** exhibited a prominent broad diffraction peak centered at 42°, which is the average of the corresponding (111) planes of the pure monometallic Cu and Pd-*fcc* structures. This observation confirmed the formation of fully alloyed bimetallic **PdCuNPs** in agreement with STEM-EDX analysis. A shoulder at 40° also suggested the presence of some Pd particles in the sample. For the **PdCu/CNTs** catalyst, a diffraction pattern very similar to that of the CNT support was observed, in agreement with the low metal loading of this catalyst (1 wt%). The absence of a sharp peak at 40° suggested the absence of monometallic PdNPs in **PdCu/CNTs** catalyst. Simulation of experimental XRD patters with ideal monometallic or bimetallic *fcc* structures (TOPAS software) permitted to calculate the experimental lattice constant for several of these nanomaterials (see Supporting Information). Interestingly, the lattice constants determined for NiCu/CNTs and PdCuNPs were very similar to the values expected for ideal $Ni_{0.5}Cu_{0.5}$ and $Pd_{0.5}Cu_{0.5}$ alloys (3.578

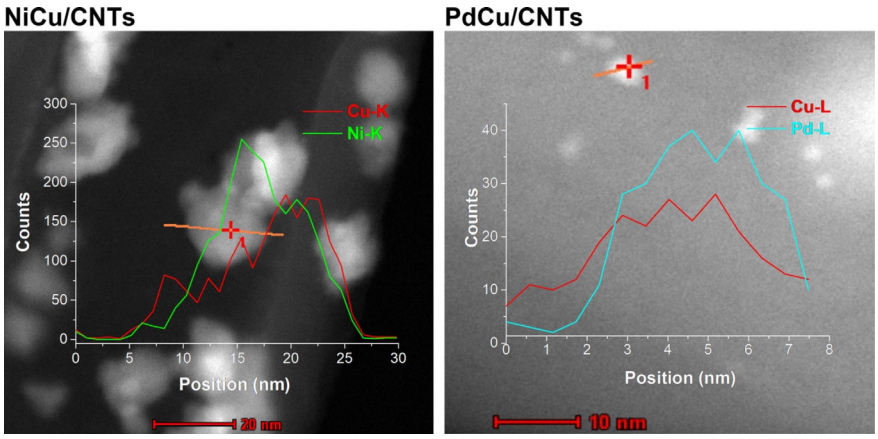


**Figure 3.** STEM-HAADF micrographs of **NiCu/CNTs** and **PdCu/CNTs** catalysts with the corresponding elemental analysis in line of single bimetallic nanoparticles.

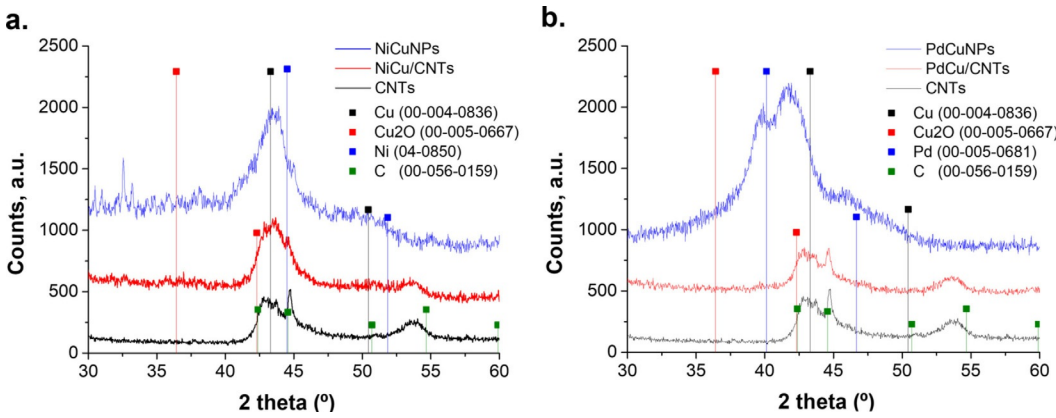


**Figure 4.** XRD analysis of colloidal and supported nanoparticles: a) NiCu; b) PdCu.

vs. 3.570, and 3.711 vs. 3.737, respectively), thus confirming the formation of fully alloyed bimetallic nanostructures.

The chemical composition and the oxidation state of the metals at the surface of the supported catalysts was studied by XPS. Microanalysis of these catalysts performed by deconvolution of full XPS spectra demonstrated the presence of nitrogen (from the carbene stabilizer) at the surface of these nanomaterials. The N content was relatively higher in the case of the copper containing catalysts than in the catalysts where copper was not present (1–2% atom/atom vs. 0.3% atom/atom, see Supporting Information).

The effect of copper alloying on the oxidation state of Pd was studied by deconvolution of Pd 3d XPS spectra (see Supporting Information). Such an analysis revealed percentages of zero valent Pd of 73% for **Pd/CNTs** and 54% in the case of **PdCu/CNTs**. In the case of the bimetallic PdCu NPs, the presence of copper could make the Pd phase more electron-deficient and may affect crucial steps of the selective alkyne hydrogenation, namely the coordination of the substrate/product and the activation of dihydrogen. Such an effect in the XPS binding energy has been previously reported for PdCu systems.[8a]

Analysis of the Cu 2p spectra of copper containing catalysts evidenced some degree of electron transfer when alloyed with Ni or Pd. For instance, comparing the Cu 2p XPS spectra of **Cu/CNTs** and **NiCu/CNTs**, it was observed a shift of 1 eV towards higher binding energies for the alloyed catalyst, possibly due to electron transfer from Cu to Ni.

The presence of the organic stabilizer in the prepared nanomaterials was studied by thermogravimetric analysis (see data in Supporting information). In general, the colloidal nanoparticles displayed weight losses of 20–45% in the range of 220–320 °C, that were attributed to the decomposition of the organic stabilizer anchored on nanoparticle surfaces. For the case of supported catalysts, the presence of NHC ligand was only detected in **NiCu/CNTs** (6–8 wt%), but not in **PdCu/CNTs** (less than 1%) due to the low metal loading in this latter case.

To determine experimental metal loadings, all the materials were analyzed by ICP-AES (Table 1).

In general, slightly lower metal loadings than nominal values were determined, in particular for copper NPs. In contrast, palladium containing catalyst displayed loadings very close to nominal values. For bimetallic catalysts, the relative percentages of the component metals were very close to the nominal

**Table 1.** Nominal and experimental metal loadings for CNTs supported catalysts.

| Catalyst | Nominal M loading, wt% | ICP-AES M loading, wt% |
|---|---|---|
| Cu/CNTs | 10.0 Cu | 6.6 Cu |
| Pd/CNTs | 1.0 Pd | 0.9 Pd |
| NiCu/CNTs | 5.0 Ni | 3.6 Ni |
| | 5.2 Cu | 3.8 Cu |
| PdCu/CNTs | 1.0 Pd | 0.8 Pd |
| | 0.7 Cu | 0.5 Cu |

values ($Ni_{0.50}Cu_{0.50}$ and $Pd_{0.47}Cu_{0.53}$ for **NiCu/CNTs** and **PdCu/CNTs**, respectively).

Summarizing, a general one-pot methodology for the preparation of a series of monometallic Cu, Pd and bimetallic NiCu and PdCu stabilized by NHC ligands was successfully employed via the in situ decarboxylation of the corresponding imidazolium carboxylate. Metal nanoparticles in the range 2–7 nm were obtained by this approach. The particle size of the colloidal nanoparticles was similar to that of the corresponding supported catalysts. Analysis of these materials by STEM–HAADF (coupled with EDX) and XRD confirmed the formation of small size metallic Cu and Pd NPs (for the case of the monometallic materials) and are in agreement with fully alloyed bimetallic NiCu and PdCu nanoparticles. The presence of NHC carbene was detected in the colloidal NPs by TGA. ICP analysis confirmed the similar nominal and experimental metal loadings and relative metal percentages on CNTs supported catalysts.

## Catalysis

### *A) Screening of catalysts*

The catalytic performance of the series of MNPs/CNT was evaluated in the semi-hydrogenation of 4-octyne (Table 2). For comparison purposes other substrates such as 1-octyne and diphenylacetylene were also tested in catalysis (see Supporting Information).

As previously reported, **Ni/CNTs** displayed excellent conversion and alkene selectivity for the hydrogenation of internal alkynes under mild conditions (3 mol% Ni, 5 bar $H_2$, 50 °C, 16 h) (entry 1),[16c] however under the same conditions this catalyst easily over-hydrogenate terminal alkynes such as 1-octyne (see Supporting Information). **Cu/CNTs** catalyst resulted inactive even using strong reaction conditions (3 mol% Cu, 50 bar $H_2$, 50 °C, 16 h). The inactivity of pure copper catalysts in the semi-hydrogenation of alkynes was also observed by other authors and mainly associated to the low activity of copper in the activation of the hydrogen molecule.[20]

In contrast, **Pd/CNTs** easily isomerize 4-octyne under very mild reaction conditions (0.1 mol% Pd, 3 bar $H_2$, 30 °C, 3 h; entry 3), showing the high activity of this metal and the associated selectivity issues. Using the bimetallic catalysts, the first observation when testing **NiCu/CNTs** was the remarkably lower activity when compared to the monometallic **Ni/CNTs** (entries 4 vs. 1). However, high conversion could be reached by increasing the reaction pressure from 5 to 50 bar while the alkene selectivity was good (93%), thus demonstrating the beneficial effect of alloying the nickel phase with copper, probably due to the more electron deficient NiCu surface.[3b] The moderation of the activity was also observed on the bimetallic **PdCu/CNTs** catalyst (entry 5). The alkene selectivity was exceptional at full conversion of the alkyne (95%), in agreement with the promoting effect of copper on the selectivity. Interestingly, under the same conditions, no over-hydrogenation was observed even after prolonged reaction times (Supporting Information).

For comparison purposes, two commercial catalysts traditionally used in the hydrogenation of liquid alkynes, namely the Lindlar and Pd Nanoselect catalysts, were also tested.[15] The palladium loadings employed were 0.05 and 0.01 mol%, for the Lindlar and Pd Nanoselect, respectively. Although full conversions were obtained (entries 6 and 7), isomerization issues were observed for both commercial references under the same reaction conditions of **PdCu/CNTs** (3 bar $H_2$, 30 °C, 0.5 h, entries 13–15).

**Table 2.** Hydrogenation of 4-octyne catalyzed by Ni, Cu, Pd, NiCu and PdCu/CNTs and commercial references.[a]

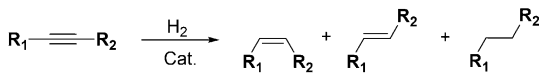


$R_1$, $R_2$ = $(CH_2)_2CH_3$ Z-A E-A B

| Entry | Catalyst | *M* [mol%][b] | *P* [bar] | *T* [°C] | *t* [h] | Conv. [%][c] | Sel. *Z*-A [%] | Sel. *E*-A/isomers, [%] | Sel. B [%] |
|---|---|---|---|---|---|---|---|---|---|
| 1[d] | **Ni/CNTs** | 3 | 5 | 50 | 16 | >99 | 99 | 0 | 1 |
| 2 | **Cu/CNTs** | 3 | 50 | 50 | 16 | – | – | – | – |
| 3 | **Pd/CNTs** | 0.01 | 3 | 30 | 3 | >99 | 66 | 31 | 3 |
| 4 | **NiCu/CNTs** | 3 | 50 | 50 | 16 | 93 | 93 | 0 | 7 |
| 5 | **PdCu/CNTs** | 0.05 | 3 | 30 | 0.5 | >99 | 95 | 4 | 1 |
| 6 | **Lindlar** | 0.05 | 3 | 30 | 0.5 | >99 | 66 | 30 | 4 |
| 7 | **Nanoselect** | 0.01 | 3 | 30 | 0.5 | >99 | 84 | 16 | 0 |

[a] Reaction conditions: 5 mL THF, 600 rpm. [b] Metal loading vs. Substrate; for bimetallic catalyst this percentage is referred to either, Ni or Pd. [c] Conversion and selectivities determined by GC-MS. [d] Reported in Ref. [16c].

### B) Effect of the PdCu composition

In view of the catalytic results obtained with the bimetallic **PdCu/CNTs** in terms of activity and resistance to over-hydrogenation, the effect of the PdCu composition was studied. For this purpose, apart from the above described monometallic Pd and Cu-nanocatalyst and the bimetallic **PdCu/CNTs** ($Pd_{0.50}Cu_{0.50}$) nanocatalysts, two additional supported bimetallic catalysts, $Pd_{0.25}Cu_{0.75}$ and $Pd_{0.75}Cu_{0.25}$ in molar fractions, were prepared and subsequently tested in the hydrogenation of 1-octyne and 4-octyne (Table 3). The employed synthetic methodology was analogous to that used for **PdCu/CNTs**, and the Pd/Cu molar ratios were adjusted accordingly (Supporting Information). The particle sizes measured for the series of PdCu NPs varied as a function of the copper content, with diameters of around 2.0 nm for Cu contents lower than 50% and of 4.4 and 6 nm for Pd0.25Cu0.75 and Pd0Cu100, respectively: $Pd_{1.00}Cu_0$ ($2.5 \pm 0.5$ nm) ≈ $Pd_{0.75}Cu_{0.25}$ ($2.1 \pm 0.4$ nm) ≈ $Pd_{0.50}Cu_{0.50}$ ($2.0 \pm 0.6$ nm) < $Pd_{0.25}Cu_{0.75}$ ($4.4 \pm 1.1$ nm.) < $Pd_0Cu_{100}$ ($6.0 \pm 1.3$ nm). The observed trend in particle size is a consequence of the competing processes of nucleation and growth which highly depend on the metal composition of the reaction mixture.

**Table 3.** Hydrogenation of 1 and 4-octyne by PdCu/CNTs supported catalysts of variable molar percentages.[a]

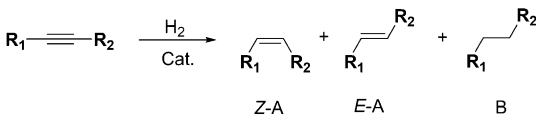


| E. | Composition mol/mol% | $R_1$ | $R_2$ | Conv, [%][b] | Sel. *Z*-A [%] | Sel. *E*-A isom. [%][c] | Sel. B [%] |
|---|---|---|---|---|---|---|---|
| 1 | $Pd_1Cu_0$ | $CH_3(CH_2)_5$ | H | >99 | 1 | 49 | 51 |
| 2 | $Pd_{0.75}Cu_{0.25}$ | $CH_3(CH_2)_5$ | H | >99 | 57 | 33 | 10 |
| 3 | $Pd_{0.50}Cu_{0.50}$ | $CH_3(CH_2)_5$ | H | **>99** | **92** | 4 | 4 |
| 4 | $Pd_{0.25}Cu_{0.75}$ | $CH_3(CH_2)_5$ | H | 22 | >99 | 0 | 0 |
| 5 | $Pd_1Cu_0$ | $CH_3(CH_2)_2$ | $CH_3(CH_2)_2$ | >99 | 80 | 18 | 0 |
| 6 | $Pd_{0.75}Cu_{0.25}$ | $CH_3(CH_2)_2$ | $CH_3(CH_2)_2$ | >99 | 97 | 1 | 2 |
| 7 | $Pd_{0.50}Cu_{0.50}$ | $CH_3(CH_2)_2$ | $CH_3(CH_2)_2$ | **99** | **95** | 4 | 1 |
| 8 | $Pd_{0.25}Cu_{0.75}$ | $CH_3(CH_2)_2$ | $CH_3(CH_2)_2$ | 18 | >99 | 0 | 0 |

[a] Reaction conditions: cat. (0.05 mol% Pd), 5 mL of dry THF, 1 bar $H_2$, 30 °C, 0.5 h. [b] Determined by GC-MS. [c] *Z*/*E* 2-octene and *E*-*A*, as isomers.

When 1-octyne was the substrate (entries 1–4), full conversions were observed for the case of the pure monometallic Pd and the bimetallic $Pd_{0.75}Cu_{0.25}$ and $Pd_{0.50}Cu_{0.50}$, while $Pd_{0.25}Cu_{0.75}$ only reached 22% of conversion under the same conditions. In terms of selectivity, palladium rich catalysts (monometallic Pd and $Pd_{0.75}Cu_{0.25}$) displayed strong over-hydrogenation and isomerization issues. The catalyst with equimolar Pd/Cu ratio ($Pd_{0.50}Cu_{0.50}$) provided 92% alkene selectivity at full conversion (entry 4) while the catalyst with lower Pd/Cu molar ratio ($Pd_{0.25}Cu_{0.75}$) reached excellent alkene selectivity (>99%) at only 22% conversion (entry 5).

Similar results were obtained in the semi-hydrogenation of 4-octyne. It was therefore concluded that low Cu contents (below 50 mol%) did not moderate appropriately the selectivity, while a high Cu content (above 50%) decreased excessively the reactivity of the palladium phase. Considering that both, terminal and internal alkynes were selectively hydrogenated by $Pd_{0.5}Cu_{0.5}$ at full conversions, this catalyst formulation was selected for subsequent studies.

Therefore, these results indicated the crucial role of the metal composition on the surface properties of bimetallic catalysts and how it affects their catalytic performance. For both substrates, the $Pd_{0.5}Cu_{0.5}$ provided excellent alkene selectivity at full conversion. Other authors have also studied the effect of the PdCu composition in the semi-hydrogenation of alkynes. For instance, Liu et al. studied the hydrogenation of phenylacetylene on PdCu/C with different Pd/Cu ratios ($Pd_{0.67}Cu_{0.33}$/C to $Pd_{0.25}Cu_{0.75}$/C). In line with our observations, the authors observed a remarkable lowering of the reaction rate for the catalysts with copper molar fractions higher to $Pd_{0.50}Cu_{0.50}$.[20] Kiwi-Minsker and co-workers studied the range between $Pd_{0.6}Cu_{0.4}$ to $Pd_{0.16}Cu_{0.84}$ for the semi-hydrogenation of dehydroisophytol (DIP). In their study, the alkene selectivity was not affected by the amount of modifier for the studied range.[8a]

### C) Evolution of reaction components over time

Next, to gain insights into the selectivity control of **PdCu/CNTs** at extended reaction times, the transformation of a series of model substrates, namely 1-octyne, 2-octyne and 4-octyne, was monitored over time (Figure 5). For this purpose, samples of the reaction crude were extracted during the first 3 h and

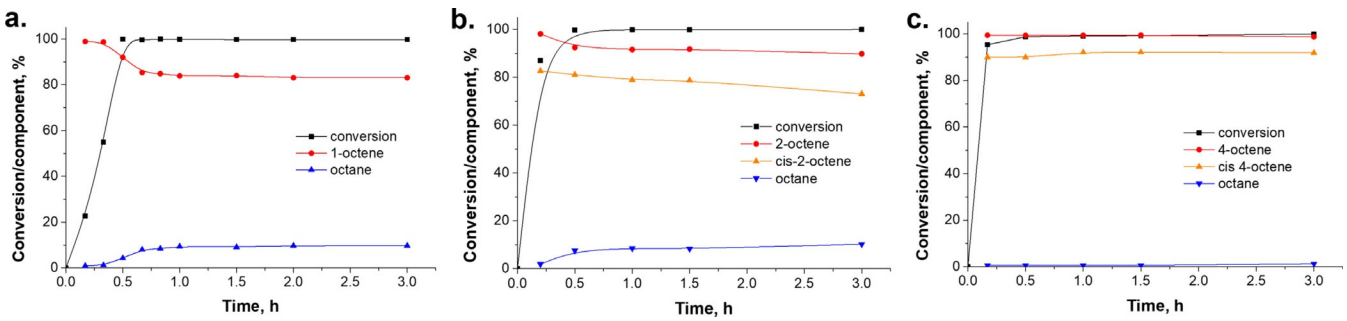


**Figure 5.** Evolution of conversion and the reaction components during the time for the semi-hydrogenation of a) 1-octyne, b) 2-octyne and c) 4-octyne catalyzed by **PdCu/CNTs**. Reaction conditions: 30 °C, 3 bar $H_2$, 0–3 h and 0.05 mol% of Pd.

the evolution of the reaction components was monitored by GC-MS. Comparing the conversion profile of the three substrates, a defined trend was identified in the reaction rate: 1-octyne < 2-octyne < 4-octyne. This observation could indicate that for **PdCu/CNTs,** the electronic properties of the substrate (or of the alkene product) may be more relevant than the steric hindrance.

Regarding the evolution of the alkene selectivity, a clear trend was also appreciable in this series: after full conversion of the alkyne (which occurs in all the cases during the first 30 min), the alkene selectivity seems to stabilize at a particular value and then remain fairly stable during the following hours without experimenting excessive over-hydrogenation. In the literature only a few examples of successful self-terminating catalytic systems for the hydrogenation of terminal alkynes (without the assistance of nitrogenated additives) have been reported to date. For instance, Mitsudome and co-workers reported total inhibition of the over-hydrogenation of terminal alkynes such as 1-octyne or phenylacetylene when using nanocatalysts based on core–shell Pd@Ag/HAC (HAC = hydroxyapatite)[8c] or Au@$CeO_2$,[21] respectively.

In this study, the alkene selectivity after 3 h of reaction increases in the following order: 1-octyne < 2-octyne < 4-octyne (80/90/99% respectively), a trend which matches the more facile over-hydrogenation of the terminal alkene product in comparison with internal alkenes.[3b]

Interestingly, the internal alkynes exhibited *Z*/*E*-isomerization at early reaction times even before of the full conversion of the alkyne. For instance, *Z*-selectivities of 80% and 90% were obtained for 2-octyne and 4-octyne at 84 and 95% of conversion, respectively. This behavior possibly indicates that the formation of the *Z*-product could follow a mechanistic selectivity pathway in which the produced *Z*-alkene is isomerized before its desorption from the metal surface.[22]

### *D) Substrate scope*

To gain more information on the reactivity of the **PdCu/CNTs** catalyst, a series of alkynes and alkynols containing various substituents such as aliphatic, aromatic or carbonyl groups were tested in the semi-hydrogenation reaction (Table 4).

For diphenylacetylene (Table 4, entries 1 and 2), 97% selectivity to the *Z* product was obtained at full conversion after 2.5 h of reaction; however, at 3 h the selectivity decreased to 90% because of *Z*/*E* isomerization. For 1-phenyl-1-butyne (entries 3 and 4) a hydrogen pressure of 6 bar was required to get reasonable hydrogenation rates and 44% conversion was obtained after 3 and 5 h of reaction, displaying the slow hydrogenation of this substrate.

The hydrogenation of phenylacetylene (entries 5 and 6) was performed with 90% selectivity at full conversion. This value remained unchanged after 3 and 5 h of reaction similarly to the observed for 1-phenyl-1-butyne. Very recently, Liu et al. reported the hydrogenation of this substrate by an activated carbon supported bimetallic catalyst ($Pd_{0.5}Cu_{0.5}$/C) at room temperature and atmospheric pressure.[20] The authors claimed that under the tested conditions the activity of this catalyst was remarkably low that reaction times above 30 h were required to approach the full conversion. The low activity was attributed to the excess of the promoter, since formulations with less copper such as $Pd_{0.67}Cu_{0.33}$/C, converted 99% of the substrate in 4 h with a 90% of alkene selectivity.

Interestingly, when 1-phenyl-2-propyn-1-ol was tested at 3 bar of $H_2$ and 3 h (entry 7), the formation of propiophenone was observed (ca. 2%) despite the low conversion of the alkynol (only 28%). Increasing the pressure from 3 to 6 bar (entry 8) allowed the full conversion of the alkynol although the alkenol selectivity dropped to 77% (with the concomitant formation of the ketone and the over-hydrogenated product

**Table 4.** Substrate scope of selective hydrogenation of alkynes and alkynols catalyzed by **PdCu/CNTs**.[a]

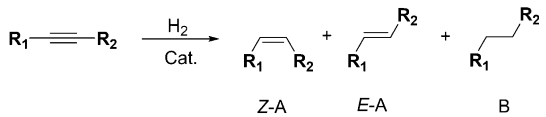


*Z*-A *E*-A B

| E. | $R_1$ | $R_2$ | Bar $H_2$ | *t* [h] | Conv. [%][b] | Sel. *Z*-A [%] | Sel. *E*-A/isom./others [%][c] | Sel. B. [c] |
|---|---|---|---|---|---|---|---|---|
| 1 | Ph | Ph | 3 | 2.5 | >99 | 97 | 0 | 3 |
| 2 | Ph | Ph | 3 | 3 | >99 | 90 | 7 | 3 |
| 3 | Ph | $CH_3CH_2$ | 6 | 3 | 43 | 87 | 5 | 8 |
| 4 | Ph | $CH_3CH_2$ | 6 | 5 | 44 | 86 | 5 | 9 |
| 5 | Ph | H | 3 | 3 | >99 | 89 | 0 | 11 |
| 6 | Ph | H | 3 | 5 | >99 | 88 | 0 | 12 |
| 7 | Ph(OH)CH | H | 3 | 3 | 28 | 98 | 2[c] | 0 |
| 8 | Ph(OH)CH | H | 6 | 3 | 99 | 77 | 8[c] | 15 |
| 9 | $CH_3(CH_2)_4$(OH)CH | H | 3 | 3 | 42 | 99 | 1[c] | 0 |
| 10 | $CH_3(CH_2)_4$(OH)CH=[d] | H | 3 | 3 | 36 | – | 9[c] | 91 |
| 11 | $CH_3(CH_2)_4$(OH)CH=[d,e] | H | 3 | 17 | 0 | – | – | – |
| 12 | $OH(CH_2)_3$ | H | 3 | 0.5 | 35 | >99 | 0 | 0 |
| 13 | $OH(CH_2)_3$ | H | 3 | 2 | >99 | 39 | 12 | 49 |
| 14 | $OH(CH_2)_2$ | $CH_3CH_2$ | 3 | 3 | >99 | 58 | 32 | 10 |
| 15 | $CH_3CH_2CO_2$ | $CH_3CH_2CO_2$ | 3 | 3 | 47 | 96 | 1 | 3 |

[a] Reaction conditions: cat. (0.05 mol% Pd), 5 mL of dry THF, 30 °C. [b] Determined by GC-MS. [c] The corresponding alkyl-ketone was observed. [d] 1-Octen-3-ol. [e] Catalyst substituted by only CNTs.

in 8 and 15%, respectively). The fast over-hydrogenation of vicinal alkynols has been already observed. For instance, Kiwi-Minsker reported the semi-hydrogenation of dehydroisophytol (DIP) catalyzed by colloidal $Pd_{0.6}Cu_{0.4}$ NPs at 4 bar $H_2$ and 80 °C. Under the tested conditions, the alkene selectivity quickly dropped when approaching the full conversion of the alkynol, showing the difficult in preventing the over-hydrogenation for these particular substrates.[8a]

In our particular case, these observations suggested that during the hydrogenation process of vicinal alkynols, the corresponding allylic alcohol products are susceptible to isomerize to the corresponding ketone. To confirm the correlation between the alkynol structure with the ketone formation, 1-octyn-3-ol was also tested at 3 bar and 3 h, resulting also in the formation of small amounts of the corresponding ketone product (1%, octan-3-one) at partial alkynol conversion (44%, entry 9, Table 4). To gain additional insights about this peculiar isomerization process, a control test employing 1-octen-3-ol was performed (as the product of partial hydrogenation of 1-octyn-3-ol) in the presence of **PdCu/CNTs** catalyst (entry 10). Under the tested conditions, 36% of the alkenol was converted into the ketone and the saturated alcohol in a 9:91 ratio, respectively, thus indicating that the isomerization or the hydrogenation of the allylic alcohol are competitive processes occurring at the NPs surface.

The palladium catalyzed isomerization of allyl alcohols to carbonyl compounds has been previously documented in the literature.[23] For instance, Young-Seok and co-workers reported the catalytic isomerization or hydrogenation of allyl alcohol catalyzed by PdNPs (in the presence of hydrogen) and the dependence of the regioselectivity with the reaction solvent or the capping agent.[23b] First, the presence of $H_2$ gas appeared to be essential for the efficient catalytic isomerization reaction thus suggesting that the mechanism involved a Pd-alkyl intermediate rather than an $\eta^3$ $\pi$-allyl Pd hydride intermediate. Regarding the effect of the solvent, in general, nonpolar or weakly polar solvents such as benzene and chloroform promoted the isomerization of allyl alcohol to propanal presumably via the formation of the branched Pd-alkyl intermediate, while, polar protic solvents such as methanol and water foster the hydrogenation to 1-propanol involving the steric induced formation of a linear Pd-alkyl intermediate.

Here, the transformation of 1-octen-3-ol into the isomerization and hydrogenation products in a 9:91 ratio (entry 10) could indicate a preferred linear coordination of the substrate on the NPs surface, possibly because of steric hindrance exerted by the carbene ligand. To discard any possible role of the CNTs in the isomerization, the same hydrogenation test was performed employing CNTs as catalyst. No isomerization was observed even after extended times (17 h, entry 11).

The reactivity of non-vicinal alkynols was also tested. For instance, the semi-hydrogenation of 4-pentyn-1-ol (entry 12, Table 4) resulted in a 35% of conversion with full selectivity towards the alkenol after 0.5 h. Curiously, lengthening the reaction time to 2 h resulted in the full conversion of the alkyne but with a considerably loss of the alkene selectivity (39%, entry 13, Table 4) due to over-hydrogenation and isomerization processes. Considering the structural similitude of this substrate with 1-octyne, the significant over-hydrogenation/isomerization issues observed for the case of the alkynol (which are absent for the case of 1-octyne) can be justified by a stronger adsorption of the alkenol product to the metal surface because of the presence of the hydroxyl group. The influence of hydroxyl groups in the reactivity of alkynols in the selective hydrogenation was previously reported by Chaudret and co-workers.[24]

This behavior was also observed when 3-hexyn-1-ol was tested (entry 14). Despite the natural resistance against over-hydrogenation or isomerization of the alkenol product, important amounts of these byproducts are observed. Finally, the semi-hydrogenation of diethyl acetylene dicarboxylate was also tested (entry 15). After 3 h of reaction, 50% conversion was observed with high alkene selectivity (96%).

### *E) Semi-hydrogenation of acetylene in the presence of ethylene*

The bimetallic **PdCu/CNTs** catalyst was evaluated in the selective hydrogenation of acetylene in the presence of ethylene. The employed reaction feed stream consisted in 1% $C_2H_2$, 20% $C_2H_4$, 5% $H_2$, 1% Ar and balance $N_2$ to roughly approximate the tail-end feed of an ethylene cracker.[25] This reaction was carried out in a micro fixed-bed reactor at 70 °C and a total pressure of 1 bar. The catalytic test was performed at iso-conversion mode at a fixed value of 70%, and then reaction parameters such as the reaction rate and selectivity were monitored during the first 40 h (for details, see the Supporting Information).[26]

The bimetallic $Pd_{0.5}Cu_{0.5}$/CNTs catalyst exhibited a stable rate of around 300 $mol_{C2H2}\,mol_{Pd}^{-1}h^{-1}$ during 40 h, demonstrating a remarkable stability under the tested reaction conditions (Figure 6). The ethylene selectivity displayed a similar profile, starting at around 60%, and then decreasing slightly during the run. Such a decrease was concomitant with a slight increase of the ethane selectivity (ca. 30%). The production of C4s was stable during the run and maintained at a value of 10%.

For comparison purposes, a commercial palladium catalyst was also tested under similar reaction conditions. The reference consisted in a $Pd/Al_2O_3$ catalyst (0.5 wt% Pd) containing PdNPs of 3 nm. Due to the very high initial activity of this monometallic Pd catalyst, the employed reaction temperature was 50 °C (in contrast to the 70 °C required for the bimetallic **PdCu/CNTs** catalyst). Although the initial activity of $Pd/Al_2O_3$ catalyst was higher compared to that of **PdCu/CNTs** (2500 vs. 1200 $mol_{C2H2}\,mol_{Pd}^{-1}h^{-1}$ respectively), it quickly decreased during the first 4 h until a value of 500 $mol_{C2H2}\,mol_{Pd}^{-1}h^{-1}$, evidencing a fast and extensive deactivation (see Supporting Information). Such a deactivation observed on Pd-based catalysts is frequently attributed to carbon deposits onto the metal surface of the PdNPs.[26] Ethylene selectivities in the range of 40–32% were registered during the run. The selectivity towards ethane and C4s was around 60 and 5% respectively.

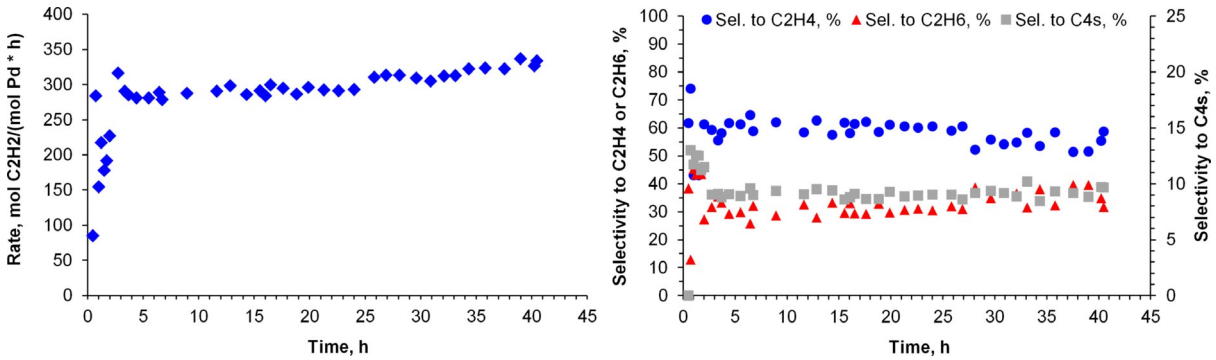


**Figure 6.** Evolution of the reaction rate and selectivities during the time obtained for **PdCu/CNTs** catalyst. Conditions: 0.1 mg Pd, 70 °C, 1 bar (iso-conversion at 70 %).

The higher performance in terms of stability and ethylene selectivity of the bimetallic **PdCu/CNTs** catalyst in comparison to the commercial reference can be ascribed to the promoting effect of the alloying copper, which exert positive geometric and electronic effects on the active Pd phase.[3b]

Previous studies have reported the promotion of palladium based catalysts with copper for the selective hydrogenation of acetylene in ethylene rich mixtures.[27] For instance, Friedrich et al. studied the effect in catalysis of disordered and ordered modifications of an unsupported $Pd_{0.40}Cu_{0.60}$ catalyst (prepared by the use or not of thermal crystallization treatments).[27a] The ordered modification corresponded to a fully alloyed structure and exhibited a high selectivity to ethylene (>90 %, 20 % higher than the disordered structure) at around 90 % conversion, and remained stable for at least 10 h on stream. The authors attributed the superior performance to the degree of ordering in the bulk crystal structure that determines the surface structure and the adsorption properties. More recently, the employment of single-atom Pd catalysts in the semi-hydrogenation of acetylene was reported.[27c,28] Pei et al. reported the application of a silica supported Cu-alloyed Pd single-atom catalyst (SAC) for the semi-hydrogenation of acetylene under simulated front-end conditions.[27c] The Cu-alloyed Pd SAC showed 85 % selectivity to ethylene at full acetylene conversion at 160 °C. Based on microcalorimetric measurements, the authors proposed that the isolation of Pd by Cu and the electron transfer from Cu to Pd not only promoted the dissociation of $H_2$ but also resulted in the weak adsorption of $C_2H_4$, giving high selectivity to ethylene at high acetylene conversion. However, it is noteworthy that relatively high reaction temperature is frequently required for this type of catalyst (>160 °C),[27c,29] in comparison to nanoparticle-based catalysts; which usually operate under milder reaction conditions.

## Conclusions

The one-pot synthetic methodology recently reported by our group for the formation of NHC-stabilized Ni-NPs was extended for the preparation of both colloidal and carbon supported monometallic Cu, Pd and bimetallic NiCu and PdCu NPs. This facile methodology demonstrated to also be useful for the variation of the PdCu composition, evidencing its robustness. These materials were fully characterized, and the alloyed structure of the bimetallic catalysts was confirmed by XRD and STEM–EDX.

From the series of catalysts, the bimetallic **PdCu/CNTs** demonstrated superior properties in the selective hydrogenation of model substrates such as 1-octyne and 4-octyne even when compared with commercial references. This result was attributed to the electronic and geometric promotion of copper in the moderation of the reactivity of the active Pd phase. The equimolar composition of $Pd_{0.5}Cu_{0.5}$ demonstrated to be the optimal for the activity and selectivity in this reaction. In terms of substrate scope, this catalyst exhibited excellent alkene selectivities for both terminal and internal alkynes bearing alkyl substituents. Alkynols underwent side reactions such as isomerization or over-hydrogenation depending on the structural characteristics of the substrate.

When **PdCu/CNTs** was evaluated in the semi-hydrogenation of acetylene in the presence of ethylene, excellent stability was observed even after 40 h of reaction with moderate to good ethylene selectivity. This result evidences the applicability of bimetallic catalysts conceived purely by colloidal techniques, not only in the semi-hydrogenation of substrates in liquid phase, but also other substrates of industrial relevance in the gas phase.

## *Acknowledgements*

The authors acknowledge the Ministerio de Economia *y* Competividad and the Fondo Europeo de Desarrollo Regional FEDER (CTQ2016-75016-R, AEI/FEDER,UE) and the Generalitat de Catalunya (SGR2014) for financial support. Authors also thank the Servei of Recursos Cientifics i Tècnics of Universitat Rovira i Virgili for the analytical assistance (specially the Unitat de Caracterització de Materials) and to the Advanced Microscopy Laboratory at Instituto de Nanociencia de Aragón for the access to STEM facilities. D.A.L.-R. is grateful for financial support (Grant 552256) by Consejo Nacional de Ciencia *y* Tecnologia (CONACYT, Mexico).

## Conflict of interest

The authors declare no conflict of interest.

**Keywords:** acetylene · alkynes · heterocycles · nanoparticles · selective hydrogenation

[1] a) P. K. Jain, X. Huang, I. H. El-Sayed, M. A. El-Sayed, *Acc. Chem. Res.* **2008**, *41*, 1578 – 1586; b) T. K. Sau, A. L. Rogach, F. Jäckel, T. A. Klar, J. Feldmann, *Adv. Mater.* **2010**, *22*, 1805 – 1825.

[2] a) A. Fedorov, H. J. Liu, H. K. Lo, C. Copéret, *J. Am. Chem. Soc.* **2016**, *138*, 16502 – 16507; b) K. Szőri, R. Puskás, G. Szőllősi, I. Bertóti, J. Szépvölgyi, M. Bartók, *Catal. Lett.* **2013**, *143*, 539 – 546; c) E. Vessally, M. Babazadeh, A. Hosseinian, S. Arshadi, L. Edjlali, *J. CO2 Util.* **2017**, *21*, 491 – 502.

[3] a) S. Cheong, J. D. Watt, R. D. Tilley, *Nanoscale* **2010**, *2*, 2045 – 2053; b) J. A. Delgado, O. Benkirane, C. Claver, D. Curulla-Ferre, C. Godard, *Dalton Trans.* **2017**, *46*, 12381 – 12403.

[4] a) R. Narayanan, M. A. El-Sayed, *J. Phys. Chem. B* **2004**, *108*, 5726 – 5733; b) R. Narayanan, M. A. El-Sayed, *Langmuir* **2005**, *21*, 2027 – 2033.

[5] a) J. Llop Castelbou, E. Bresó-Femenia, P. Blondeau, B. Chaudret, S. Castillón, C. Claver, C. Godard, *ChemCatChem* **2014**, *6*, 3160 – 3168; b) A. Reina, I. Favier, C. Pradel, M. Gómez, *Adv. Synth. Catal.* **2018**, *360*, 3544 – 3552.

[6] N. López, C. Vargas-Fuentes, *Chem. Commun.* **2012**, *48*, 1379 – 1391.

[7] a) D. Mei, M. Neurock, C. M. Smith, *J. Catal.* **2009**, *268*, 181 – 195; b) M. García-Mota, J. Gómez-Díaz, G. Novell-Leruth, C. Vargas-Fuentes, L. Bellarosa, B. Bridier, J. Pérez-Ramírez, N. López, *Theor. Chem. Acc.* **2011**, *128*, 663 – 673; c) F. Studt, F. Abild-Pedersen, T. Bligaard, R. Z. Sørensen, C. H. Christensen, J. K. Nørskov, *Science* **2008**, *320*, 1320 – 1322; d) E. Vignola, S. N. Steinmann, B. D. Vandegehuchte, D. Curulla, P. Sautet, *J. Phys. Chem. C* **2016**, *120*, 26320 – 26327.

[8] a) A. Yarulin, I. Yuranov, F. Cárdenas-Lizana, D. T. L. Alexander, L. Kiwi-Minsker, *Appl. Catal. A* **2014**, *478*, 186 – 193; b) C. F. Calver, P. Dash, R. W. J. Scott, *ChemCatChem* **2011**, *3*, 695 – 697; c) T. Mitsudome, T. Urayama, K. Yamazaki, Y. Maehara, J. Yamasaki, K. Gohara, Z. Maeno, T. Mizugaki, K. Jitsukawa, K. Kaneda, *ACS Catal.* **2016**, *6*, 666 – 670.

[9] a) L. M. Bronstein, D. M. Chernyshov, I. O. Volkov, M. G. Ezernitskaya, P. M. Valetsky, V. G. Matveeva, E. M. Sulman, *J. Catal.* **2000**, *196*, 302 – 314; b) E. Sulman, V. Matveeva, A. Usanov, Y. Kosivtsov, G. Demidenko, L. Bronstein, D. Chernyshov, P. Valetsky, *J. Mol. Catal. A* **1999**, *146*, 265 – 269; c) S. Wang, Z. Xin, X. Huang, W. Yu, S. Niu, L. Shao, *Phys. Chem. Chem. Phys.* **2017**, *19*, 6164 – 6168.

[10] M. Ren, C. Li, J. Chen, M. Wei, S. Shi, *Catal. Sci. Technol.* **2014**, *4*, 1920 – 1924.

[11] C. W. A. Chan, A. H. Mahadi, M. M.-J. Li, E. C. Corbos, C. Tang, G. Jones, W. C. H. Kuo, J. Cookson, C. M. Brown, P. T. Bishop, S. C. E. Tsang, *Nat. Commun.* **2014**, *5*, 5787.

[12] N. Kaeffer, H. J. Liu, H. K. Lo, A. Fedorov, C. Copéret, *Chem. Sci.* **2018**, *9*, 5366 – 5371.

[13] A. Shaygan Nia, S. Rana, D. Döhler, F. Jirsa, A. Meister, L. Guadagno, E. Koslowski, M. Bron, W. H. Binder, *Chem. Eur. J.* **2015**, *21*, 10763 – 10770.

[14] A. Jung, A. Jess, T. Schubert, W. Schütz, *Appl. Catal. A* **2009**, *362*, 95 – 105.

[15] G. Vilé, N. Almora-Barrios, S. Mitchell, N. López, J. Pérez-Ramírez, *Chem. Eur. J.* **2014**, *20*, 5926 – 5937.

[16] a) J. Hori, K. Murata, T. Sugai, H. Shinohara, R. Noyori, N. Arai, N. Kurono, T. Ohkuma, *Adv. Synth. Catal.* **2009**, *351*, 3143 – 3149; b) L. Montiel, J. A. Delgado, M. Novell, F. J. Andrade, C. Claver, P. Blondeau, C. Godard, *ChemCatChem* **2016**, *8*, 3041 – 3044; c) M. D. de los Bernardos, S. Perez-Rodriguez, A. Gual, C. Claver, C. Godard, *Chem. Commun.* **2017**, *53*, 7894 – 7897.

[17] N. Karousis, G. E. Tsotsou, F. Evangelista, P. Rudolf, N. Ragoussis, N. Tagmatarchis, *J. Phys. Chem. C* **2008**, *112*, 13463.

[18] W. H. Qi, M. P. Wang, Y. C. Su, *J. Mater. Sci. Lett.* **2002**, *21*, 877 – 878.

[19] T. Ohba, H. Kubo, Y. Ohshima, Y. Makita, N. Nakamura, H. Uehara, S. Takakusagi, K. Asakura, *Bull. Chem. Soc. Jpn.* **2017**, *90*, 720 – 727.

[20] J. Liu, Y. Zhu, C. Liu, X. Wang, C. Cao, W. Song, *ChemCatChem* **2017**, *9*, 4053 – 4057.

[21] T. Mitsudome, M. Yamamoto, Z. Maeno, T. Mizugaki, K. Jitsukawa, K. Kaneda, *J. Am. Chem. Soc.* **2015**, *137*, 13452 – 13455.

[22] Á. Molnár, A. Sárkány, M. Varga, *J. Mol. Catal. A* **2001**, *173*, 185 – 221.

[23] a) E. Sadeghmoghaddam, K. Gaïeb, Y. S. Shon, *Appl. Catal. A* **2011**, *405*, 137 – 141; b) E. Sadeghmoghaddam, H. Gu, Y. S. Shon, *ACS Catal.* **2012**, *2*, 1838 – 1845.

[24] V. Kelsen, B. Wendt, S. Werkmeister, K. Junge, M. Beller, B. Chaudret, *Chem. Commun.* **2013**, *49*, 3416 – 3418.

[25] a) Y. Zhang, W. Diao, J. R. Monnier, C. T. Williams, *Catal. Sci. Technol.* **2015**, *5*, 4123 – 4132; b) Y. Zhang, W. Diao, C. T. Williams, J. R. Monnier, *Appl. Catal. A* **2014**, *469*, 419 – 426.

[26] A. Pachulski, R. Schödel, P. Claus, *Appl. Catal. A* **2011**, *400*, 14 – 24.

[27] a) M. Friedrich, S. A. Villaseca, L. Szentmiklósi, D. Teschner, M. Armbrüster, *Materials* **2013**, *6*, 2958 – 2977; b) S. Leviness, V. Nair, A. H. Weiss, Z. Schay, L. Guczi, *J. Mol. Catal.* **1984**, *25*, 131 – 140; c) G. X. Pei, X. Y. Liu, X. Yang, L. Zhang, A. Wang, L. Li, H. Wang, X. Wang, T. Zhang, *ACS Catal.* **2017**, *7*, 1491 – 1500.

[28] X. Huang, Y. Xia, Y. Cao, X. Zheng, H. Pan, J. Zhu, C. Ma, H. Wang, J. Li, R. You, S. Wei, W. Huang, J. Lu, *Nano Res.* **2017**, *10*, 1302 – 1312.

[29] F. Huang, Y. Deng, Y. Chen, X. Cai, M. Peng, Z. Jia, P. Ren, D. Xiao, X. Wen, N. Wang, H. Liu, D. Ma, *J. Am. Chem. Soc.* **2018**, *140*, 13142 – 13146.

Manuscript received: March 5, 2019
Revised manuscript received: April 17, 2019
Accepted manuscript online: April 23, 2019
Version of record online: May 22, 2019